Title	Interconnected pores on the walls of a polymeric honeycomb monolith structure created by the unidirectional freezing of a binary polymer solution
Author(s)	Okaji, Rika; Sakashita, Shota; Tazumi, Kohei; Taki, Kentaro; Nagamine, Shinsuke; Ohshima, Masahiro
Citation	Journal of Materials Science (2013), 48(5): 2038-2045
Issue Date	2013-03
URL	http://hdl.handle.net/2433/189835
Right	The final publication is available at Springer via http://dx.doi.org/10.1007/s10853-012-6973-2
Type	Journal Article
Textversion	author

Interconnected Pores on the Walls of a Polymeric Honeycomb Monolith Structure Created by the Unidirectional Freezing of a Binary Polymer Solution.

Rika Okaji, Shota Sakashita, Kohei Tazumi, Kentaro Taki, Shinsuke Nagamine, Masahiro Ohshima*

Department of Chemical Engineering, Kyoto University, Kyoto 615-8510, Japan

*Corresponding author. Tel.: +81 75 383 2666, fax: +81 75 383 2646

Email: oshima@cheme.kyoto-u.ac.jp

Abstract

Interconnected submicron pores were created on the walls of a honeycomb monolith structure by the unidirectional freezing of a binary polymer solution. Agglomerated globules of polyethylene glycol (PEG) in a binary solution of polystyrene (PS) and PEG in 1,4-dioxane solvent were frozen unidirectionally in a liquid nitrogen bath. Removing the frozen solvent and the agglomerated globules of PEG by freeze-drying and leaching, respectively, enabled us to create interconnected pores in the PS walls. The combination of PS and PEG was effective in creating interconnected pores in the walls because PS and PEG are poorly soluble in one another. The higher freezing rate and lower PEG weight fraction of the binary solution effectively reduced the pore size in the microtube walls.

Keywords: Porous material; honeycomb monolith structure; unidirectional freezing;

freeze-drying; phase separation.

Introduction

Honeycomb monolith structures have garnered significant scientific interest because of their unique porous structure. Unidirectional freezing and freeze-drying was used to form porous materials with a micrometer-sized honeycomb structure comprised of highly ordered microtubes that align in the freezing direction[1-4]. This unidirectional freezing and freeze-drying method has been applied to various materials, such as polymer solutions[4-8], solgels[9-12], hydrogels[13], ceramic slurries[11, 14-20], and inorganic particles in colloidal solutions[2, 12, 21]. Because of their highly porous structure, they have been used as catalyst supports[13], catalysts[12], drug delivery media[22], and bioscaffolds[7].

Unidirectional freezing is a highly controllable process. Well-defined porous structures can be achieved by varying the freezing rate[14, 23, 24], material concentration[5, 15], and particle size of a ceramic slurry[25] and by adding impurities to the solution[4, 6]. Current honeycomb monolith structures exhibit poor interconnectivity through the microtube walls, which can cause plug flow, lower contact efficiency and a higher pressure drop. Kim et al[6] successfully prepared a porous honeycomb monolith structure with interconnecting microtube walls from a binary polymer solution of poly(L-lactic acid) (PLLA) and PEG in 1,4-dioxane (Dx) solvent, in which PEG was the porogen and PLLA was the base matrix, using unidirectional freezing and porogen leaching methods. In their study, the following pore formation mechanism was proposed. The Dx concentration in solution decreased as it crystallized during the unidirectional freezing

process. At a certain Dx concentration, the solvent crystals trapped the polymers (PLLA and PEG) in a crystalline morphology characterized by PEG islands surrounded by PLLA. Leaching the PEG domains resulted in the formation of interconnected pores in the microtube walls.

Several studies have reported on the ability of solvent evaporation to induce phase separations in a binary polymer solution before solidification, forming porous membranes[26, 27]. Kim et al.[26] prepared a polymeric porous film from a binary polymer solution of polystyrene (PS), poly(ethylene glycol) (PEG), and toluene solvent by dry-casting. The polymer solution was cast on an aluminum Petri dish and allowed to dry in a temperature-controlled and nitrogen-purged incubator. The obtained films exhibited micron-scale pores (approximately 12 μm) that had formed without leaching the PEG-droplets. The researchers suggested that the pores were formed by polymer-polymer phase separations and PEG-solvent phase separations in the PEG phase.

These studies found that decreasing the solvent concentration induced polymer demixing. Kim et al[6] used a binary polymer solution of PS and PEG in toluene, which is difficult to apply to unidirectional freezing due to the lower freezing point of toluene. Nevertheless, their study suggests a method for creating pores in the walls of honeycomb monolith structure. In studies on unidirectional freezing, Kim et al[6] used 1,4-dioxane as a solvent because of the large cryoscopic constant and high vapor

pressure of the crystal. Therefore, a dry-casting experiment with PS/PEG/Dx binary polymer solution was used to confirm the structure formation via polymer demixing.

Figure 1 shows SEM micrographs of the films made by solvent drying from both PS/PEG/Dx and PLLA/PEG/Dx solutions using the same method as Kim et al[26]. The ratios of binary polymers, PS/PEG and PLLA/PEG, were 70/30, and the total concentration of binary polymers was 10 wt. %. The solutions were dried under a 3 L/min N_2 purge. As observed in Figure 1, a greater number of micron-scale pores were formed on the PS/PEG film surfaces than those of the PLLA/PEG/Dx binary polymer solution. It was instructive that PS was better suited to create pores than PLLA when paired with PEG. Styrene is less compatible with ethylene glycol than lactic acid is[28]. Selecting the pair of less soluble polymers is key for creating pores via phase separation induced by solvent evaporation.

In this study, the binary polymer of PS and PEG in Dx solvent was subjected to unidirectional freezing to create numerous pores on the walls of the honeycomb monolith structures. The in-situ cloud and freeze points were measured to understand the time-course of the agglomeration of polymer domains and the freezing of the solvent. The dynamic light scattering (DLS) technique was also employed to investigate the size of polymer domains to determine which polymer droplet was formed during unidirectional freezing.

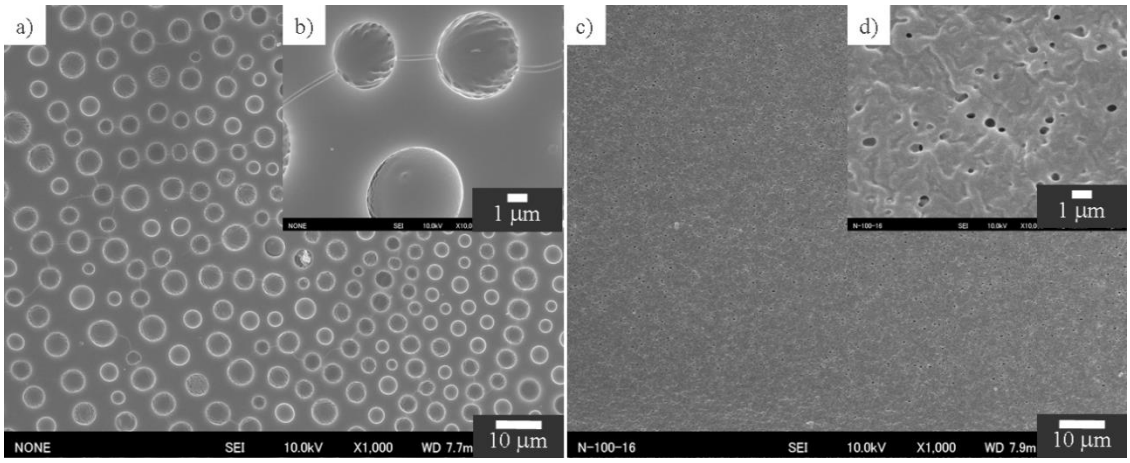

Figure 1 Surfaces of PS/PEG and PLLA/PEG films prepared by solvent evaporation. The solvent was Dx, and the total polymer concentration was 5 wt. % in each solution.

Experimental

Materials

PS (Polystyrene, Mw = 280,000 g/mol, Aldrich) and PEG (polyethylene glycols, Mw = 20,000 g/mol, Wako Chemicals Ind. Ltd.) were used as the polymers, and dehydrated 1,4-dioxane (Dx, Wako Chemicals Ind. Ltd.) was used as the solvent. PS and PEG were dissolved in Dx at 313 K. Prior to dissolution, PS and PEG were dried in a vacuum oven for 1 day to remove moisture. The solutions were prepared at total polymer concentrations of 5, 7, and 10 wt. % and PS and PEG blend ratios of 70/30 and 90/10, respectively.

Unidirectional Freezing Process

The procedural details for unidirectional freezing were found elsewhere[6]. In brief, the binary polymer solution was poured into polypropylene (PP) test tubes with the following dimensions: 1.2-mm-thick walls, 10-mm diameter, and 100-mm length. The solution in the PP test tubes was unidirectionally frozen by immersion in a liquid nitrogen bath at 1.5, 3.5, and 7.0 cm/hr. The frozen samples were freeze-dried at 253 K for 4 days *in vacuo*, and the PEG was leached in distilled water over 7 days. After leaching the PEG from the material, the samples were dried under vacuum for an additional 4 days. The obtained porous honeycomb structure consisted primarily of PS.

Characterization

Scanning electron microscopy (SEM, upgraded Tiny-SEM 1540, Technex Lab Co. Ltd., Japan) was used to image the obtained cell structures. The SEM preparation scheme was the same as in our previous paper[6].

Dynamic Light Scattering (DLS) Measurement

Light scattering measurements were performed on a Zetasizer Nano ZS (Malvern, UK). This technique measures the diffusion of particles moving under Brownian motion, which is then converted into a particle size and size distribution using the Stokes-Einstein relationship. The measurement was performed for the individual 5 wt. % PS and PEG polymer solutions and the 7 wt. % PS/PEG (= 70/30) solution in Dx solvent at 20°C.

In Situ Cloud and Freeze Point Measurement

An in situ cloud and freeze point measurement was conducted to investigate the relationship between polymer agglomeration and the freeze point of the sample solution. A simple laser transmittance apparatus was used to measure the turbidity and temperature of solutions with various total polymer concentrations and polymer blend ratios. The solution temperature was lowered from 20°C at a rate of 0.7°C/min. Details of the measurement scheme can be found in previous work[6].

Results and Discussion

Porous structure prepared by unidirectional freezing

The binary polymer solution of 70/30 PS/PEG in Dx solvent with a total polymer concentration of 7 wt. % was frozen unidirectionally at an immersion rate of 3.5 cm/h into the liquid nitrogen bath. Figures 2 (a-c) show the SEM micrographs of the honeycomb monolith structure obtained before leaching PEG in water. The cellular-honeycomb monolith structure was characterized by microtubes with diameters of approximately 10 ~ 20 μm and nano-scale pores up to 300 nm in diameter in the microtube walls. The nano-scale pores were formed by the sublimation of Dx crystals in the agglomerated PEG-globules.

The results of unidirectionally freezing the PS/PEG/Dx solution indicate that the preliminary experiment was helpful for selecting PS as the polymer to be paired with PEG. To create more pores on the walls, the microtube walls of Figure 2 (c) were immersed in distilled water to leach out the PEG domains from the walls. The formation of a greater number of pores on the microtube walls is apparent in Figure 2 (d) relative to Figure 2 (c). The results indicate that most of the agglomerated PEG-globules were embedded in the microtube walls.

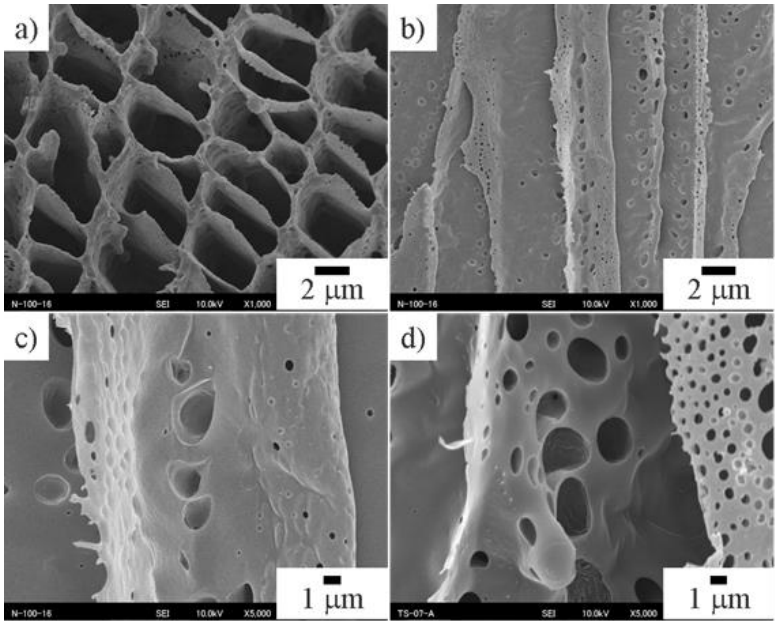

Figure 2 SEM micrographs of the honeycomb monolith structures obtained by unidirectional freezing followed by freeze-drying PS/PEG20000/Dx with a 70/30 (w/w) ratio of PS to PEG. (a): cross section perpendicular to the freezing direction, (b): cross section parallel to the freezing direction (c): magnified view of (b). (d): magnified view of the sample after leaching with water.

As mentioned above, most of the pores on the microtube walls were exposed by leaching out the agglomerated PEG-globules. To confirm the existence of the agglomerated PEG-globules in the solution, dynamic light scattering (DLS) and in situ cloud point and freeze point measurements were performed. The dynamic light scattering measurement gives the hydrodynamic diameter (D_H) of the suspension, which could be characterized as either a globule of polymer chains or an agglomeration of polymer domains, depending on the diameter.

Figure 3 shows the distributions of the hydrodynamic diameters of (a) 5 wt. % PS, (b) 2.1 wt. % PEG and (c) 7 wt. % PS/PEG, whose polymer ratio was 70/30. As shown in Figures 3 (a, b), the PEG/Dx solution has two distinct D_H peaks, whereas the PS/Dx solution has only one peak. The peak at approximately 10 nm for both solutions originates from globules of the PS and PEG chains. PS exhibited a higher D_H than PEG because of its higher molecular weight. Moreover, according to the Hansen solubility parameters, Dx is a good solvent for PS and a poor solvent for PEG. The PS polymer chain is more swollen than that of PEG.

Another peak at 373 nm in the PEG/Dx solution could be attributed to spherical domains formed by the agglomeration of the PEG globules. Once the PEG globules form the spherical domain of agglomerated PEG-globules, their hydrodynamic diameter becomes fairly large. The Brownian motion of the agglomerated PEG decreases.

Figure 3 (c) shows the D_H distribution of the PS/PEG binary polymer solution (7

wt. %, 70/30) in Dx solvent, which has two distinct peaks at 5.84 nm and 93.7 nm. These peaks are assigned to the polymer chain globules and the spherical domains of agglomerated globules, respectively. Because PS polymer chains are dispersed in the good solvent, they tend not to agglomerate, instead forming a large domain at this concentration. As the PEG chains tend to form spherical domains of agglomerated PEG, the larger peak in Figure 3 (c) at 93.7 nm consists of a large number of agglomerated PEG globules.

The spherical domain of agglomerated PEG is 373 nm in the unary solution and 93.7 nm in the PEG/PS binary polymer solution. The decrease of D_H from 373 to 93.7 nm is caused by the adsorption of the PS chain on the spherical domains of PEG. The PS chains reduced the electrostatic interaction between the PEG chains and the solvent, allowing much smaller spherical domains to exist in PS/PEG/Dx.

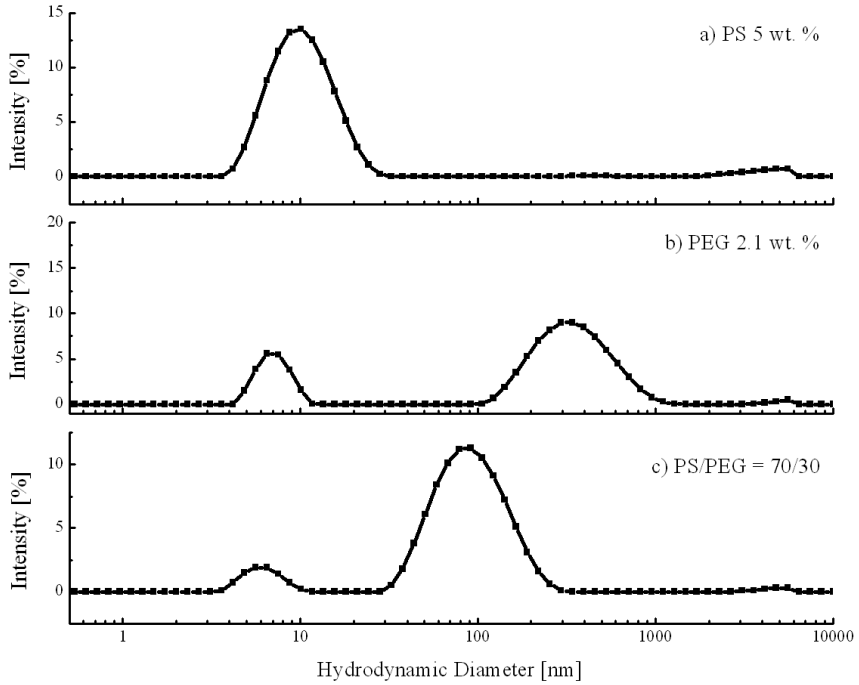

Figure 3 Results of the DLS measurement under 20 °C of (a) 5 wt. % PS, (b) 2.1 wt. % PEG, and (c) 7 wt. % PS/PEG (= 70/30) in Dx solvent.

Figure 4 shows the temperature-time and laser intensity-time curves of the binary polymer solution acquired during the cloud point and freeze point measurements. The PS/PEG blend ratio was 70/30, and the total polymer concentration was 7 wt. %. Because of the heat of fusion of Dx, a temperature increase was observed with the occurrence of solvent crystallization. At this point, the generated solvent crystals scattered the laser light, reducing the transmitted intensity.

A small intensity decline without a temperature increase was observed before the freeze point, indicating that the agglomeration of PEG-globules occurred in solution and scattered the light at low temperatures.

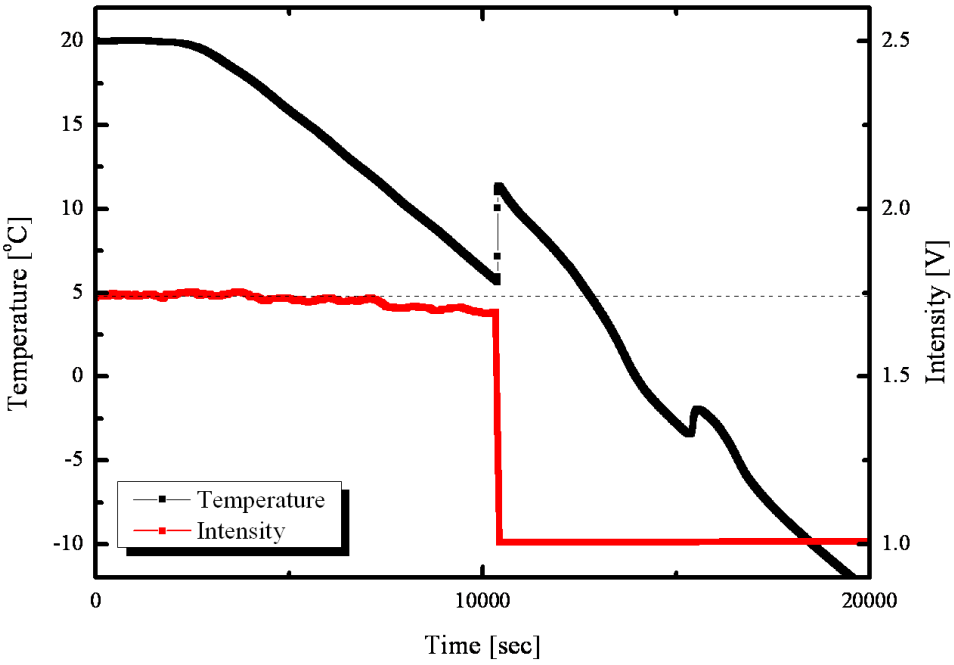

Figure 4 Cloud and freeze point measurements of the PS/PEG/Dx solution. The total polymer concentration was 7 wt. %, and the PS/PEG blend ratio was 70/30. Black, temperature-time profile; red, laser intensity profile. The horizontal dashed line is the initial laser intensity.

The pore size distributions obtained from Figures 2 (c, d) are shown in Figure 5. The changes in the pore size distribution before and after PEG leaching are clearly observed. The leaching of the PEG phase increased the number of interconnected pores in the walls. The average pore size before PEG leaching was 1.63 μm, and the average for size after the leaching was 1.26 μm. Most of the newly observed pores have smaller diameters than the previously existing pores. These tiny pores had not only been filled but also covered by the PEG globules, which precipitated at the interface of the solvent crystals and formed a thin cover layer that could be removed by leaching.

In the following sections, the SEM micrographs of the porous samples and the average pore sizes on the wall refer to observations after the leaching process. The effects of the freezing rate and PEG weight fraction in solution on the pore diameters on the microtube walls were investigated to understand the cause-and-effect relationships of the unidirectional freezing of a binary polymer solution.

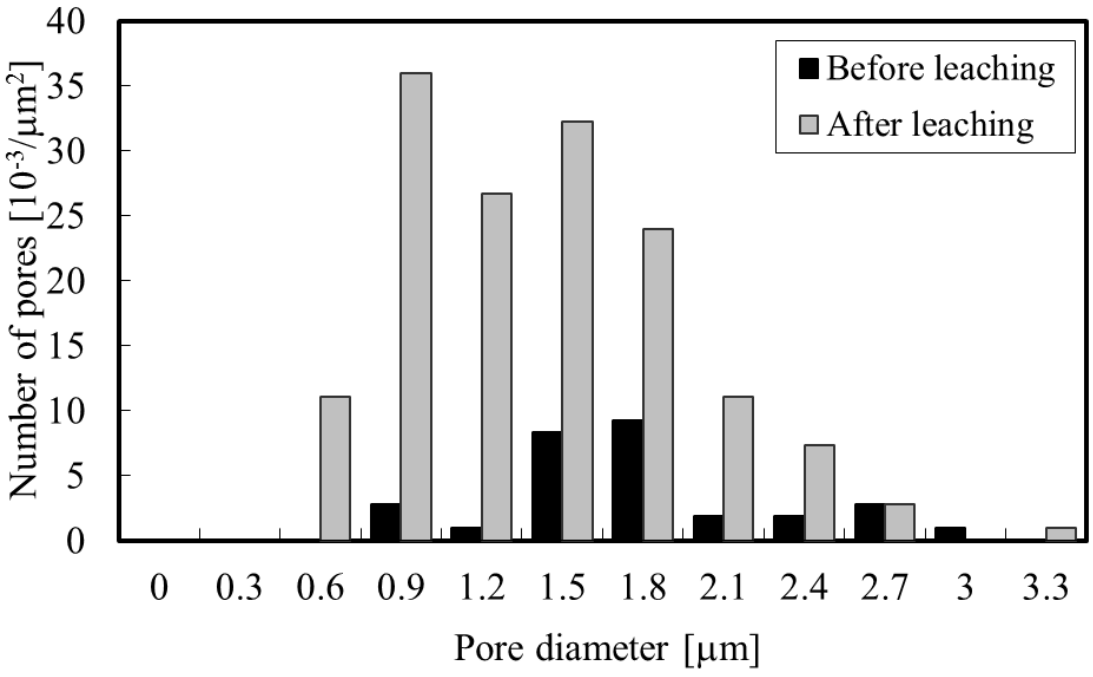

Figure 5 Pore diameter distribution before and after the leaching of PEG.

Effects of freezing rate on pores in the microtube walls

The unidirectional freezing series was conducted at three different freezing rates while maintaining a 70/30 blend ratio and a total polymer concentration of 7 wt. %. The examined freezing rates were 1.5, 3.5, and 7.5 cm/hr. Figures 6 (a-c) show that cellular honeycomb monolith structures were obtained at all freezing rates. The pore sizes on the microtube walls at different freezing rates are plotted in Figure 7. The pore diameter is on the order of microns at 1.5 and 3.5 cm/hr and submicrons at 7.5 cm/h. The pore size in the microtube walls decreased with increasing freezing rate. The pore size could be adjusted by tuning the freezing rate, which changes the agglomeration time of the spherical domains of the PEG-phase until the freeze point.

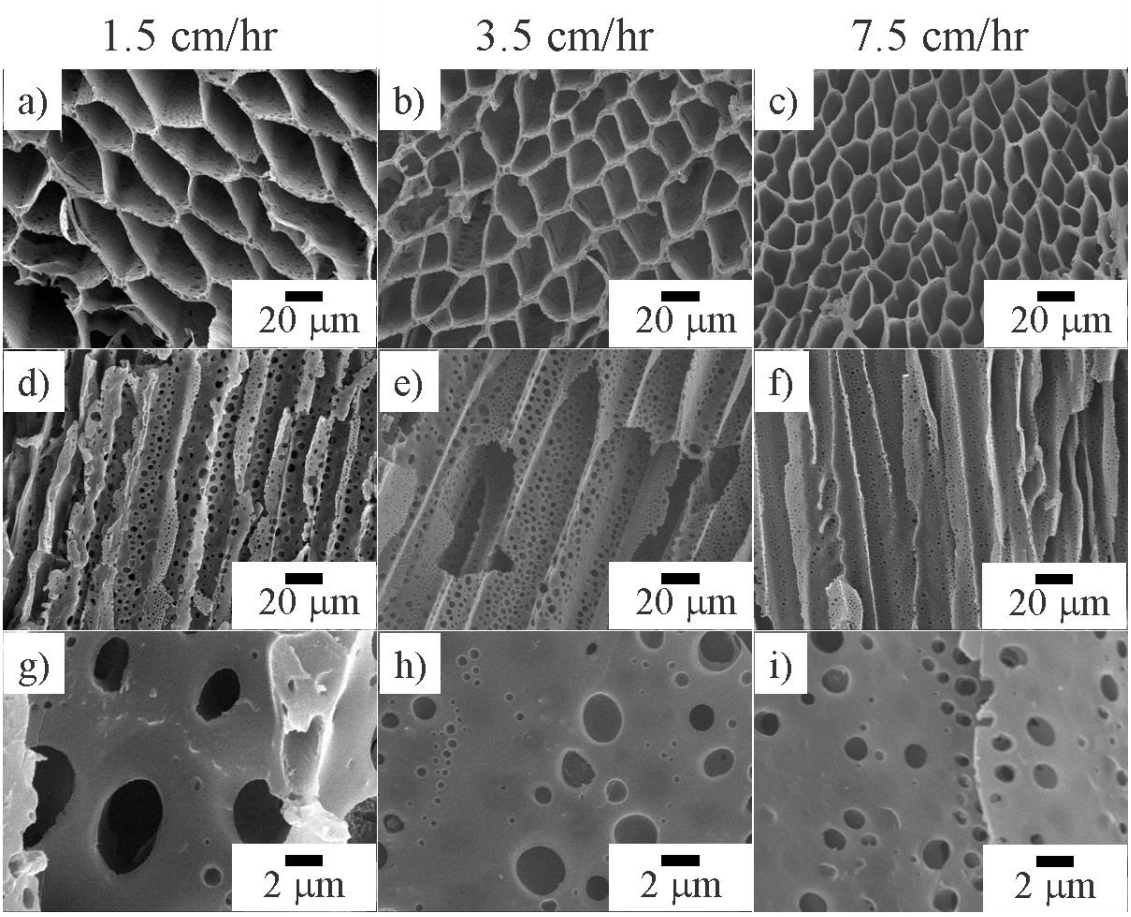

Figure 6 Effects of freezing rate on the honeycomb structure and pores on the tube walls. (a-c): cross-sections perpendicular to the freezing direction, (d-f): cross-sections parallel to the freezing direction, (g-i): the porous tube wall at higher magnification. Immersion rates: (a, d, g) 1.5, (b, e, h) 3.5, and (c, f, i) 7.5 cm/h. PS/PEG ratio =70/30.

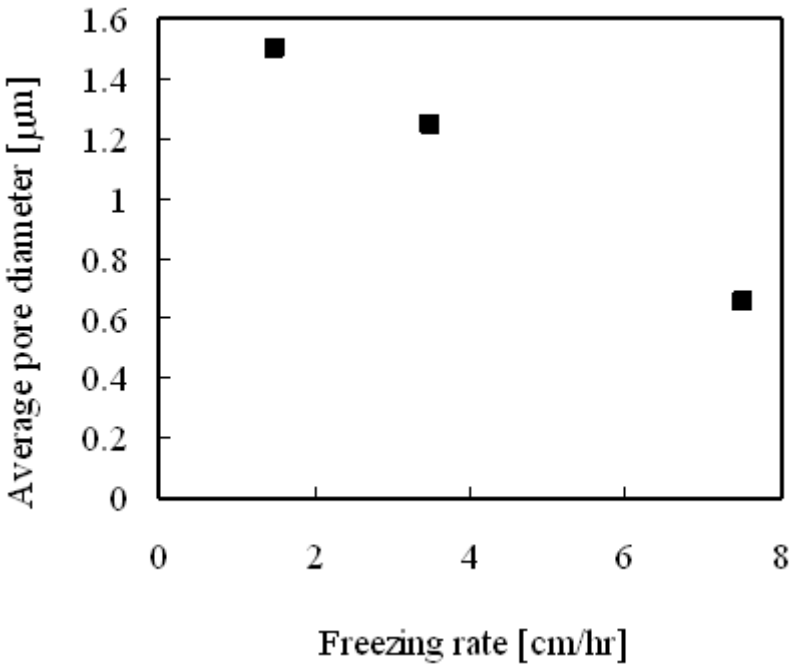

Figure 7 Changes in pore diameter with freezing rate. Total polymer concentration = 7 wt. %, PS/PEG blend ratio = 70/30.

Effects of the Total Polymer Concentration or PS/PEG Blend Ratios on the Microscale Pores on the Microtube Walls

To investigate the effect of total polymer concentrations or PS/PEG blend ratios on the pores on the microtube walls, solutions of PS/PEG/Dx at different total polymer concentrations at different PS/PEG blend ratios were prepared and unidirectionally frozen.

Figure 8 shows SEM micrographs of the samples prepared at a constant immersion rate of 3.5 cm/hr. Cellular honeycomb structures with microtubes characterized by smooth walls and pores were observed in the samples containing total polymer concentrations of 5 and 7 wt. %. In contrast, dendrite structures emerged when the total polymer concentration was increased to 10 wt. % due to the increased instability of the solvent crystalline growth. The pores on the walls derived from PEG agglomeration are larger for higher total polymer concentrations and PEG blend ratios. The pore size varied with the total amount of the source of the spherical domains in the PEG phase.

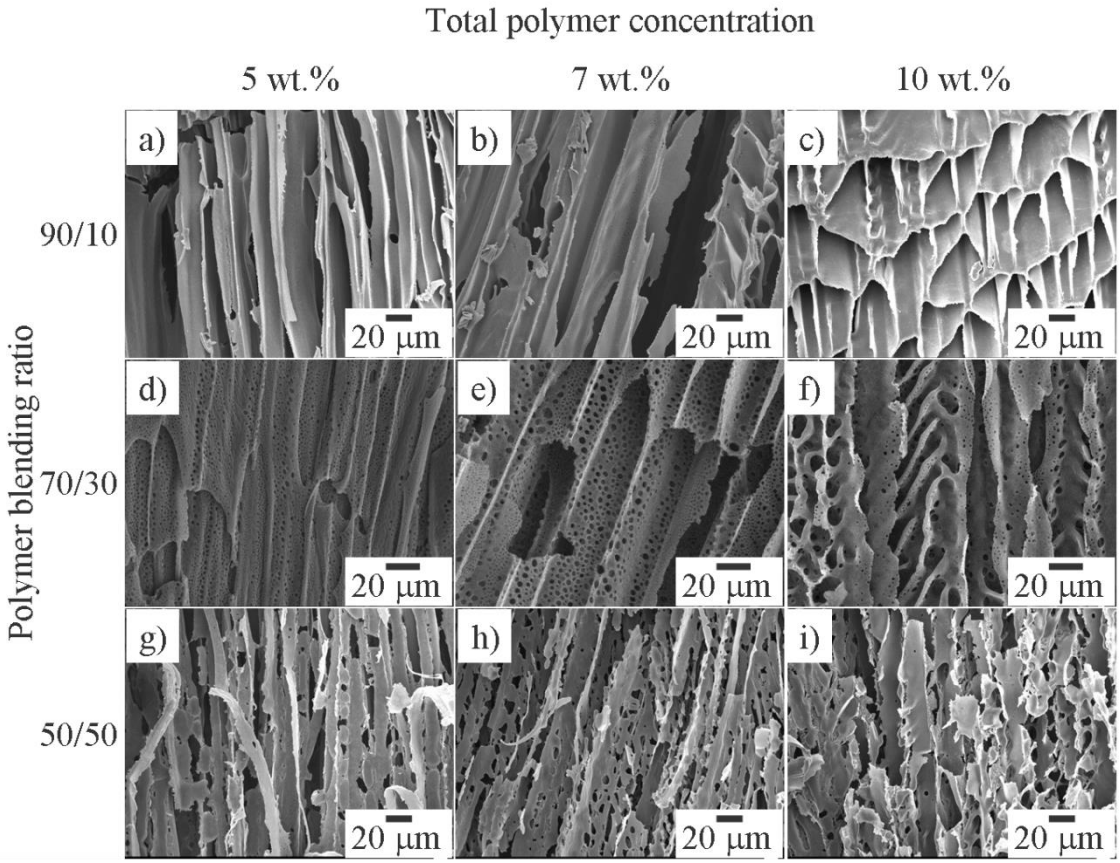

Figure 8 Effect of total polymer concentration and PS/PEG blend ratio on the micron-sized pores on the honeycomb walls.

Conclusions

The binary polymer solution of PS and PEG in Dx solvent was applied to the unidirectional freezing process to create interconnected pores in the microtube walls of the honeycomb monolith structure.

Micrometer- and submicrometer-sized pores were successfully created on the walls. The pore size could be varied by changing the freezing rate and the total polymer concentration of PS and PEG.

The cloud and freeze point measurements and the dynamic light scattering indicate the existence of spherical domains of agglomerated PEG before solvent freezing. These domains tended to increase the size of the agglomerates, which is key in controlling the size of the PEG phase and eventually determining the pore size.

Appendix.

The Hansen solubility parameter (HSP) predicts that styrene is less compatible with ethylene glycol than lactic acid is[28]. HSP is based on the idea that "like dissolves like," wherein one molecule is considered to be "like" another if it bonds to itself in a similar way. Specifically, each molecule is given three individual parameters, each of which is generally measured in $MPa^{0.5}$ in Hansen parameters: the energy from dispersion forces (δ_D), the energy from dipole moment forces (δ_P), and the energy from hydrogen bond forces (δ_H). The HSPs of each molecule used in this study are listed in Table 1 and plotted on a 3-D coordinate system known as Hansen space in Figure 9. In Hansen space, the nearer two molecules are, the more likely they are to dissolve into each other. The distance between two molecules is calculated using equation (1), where the constant "4" was found to be convenient and correctly represented the solubility data.

$$(Ra)^2 = 4(\delta_{D2}^2 - \delta_{D1}^2) + (\delta_{P2}^2 - \delta_{P1}^2) + (\delta_{H2}^2 - \delta_{H1}^2) \quad (1)$$

The calculated Ra values between Dx and each polymer unit and between ethylene glycol and each polymer unit are listed in Table 1. This result indicates that ethylene glycol has poorer miscibility into styrene than into lactic acid.

Table 1 Hansen solubility parameters of each molecules at 25 °C.[引用:HSP)]

	δ_D [$MPa^{0.5}$]	δ_P [$MPa^{0.5}$]	δ_H [$MPa^{0.5}$]	R_a (-Dx)	R_a (-EG)
1,4-Dioxane	19.6	1.8	7.4	---	---
Styrene	18.6	1.0	4.1	15.53	589.85
(D, L-) Lactic acid	17.0	8.3	28.4	510.29	13.05
Ethylene glycol	17.0	11.0	26.0	457.64	---

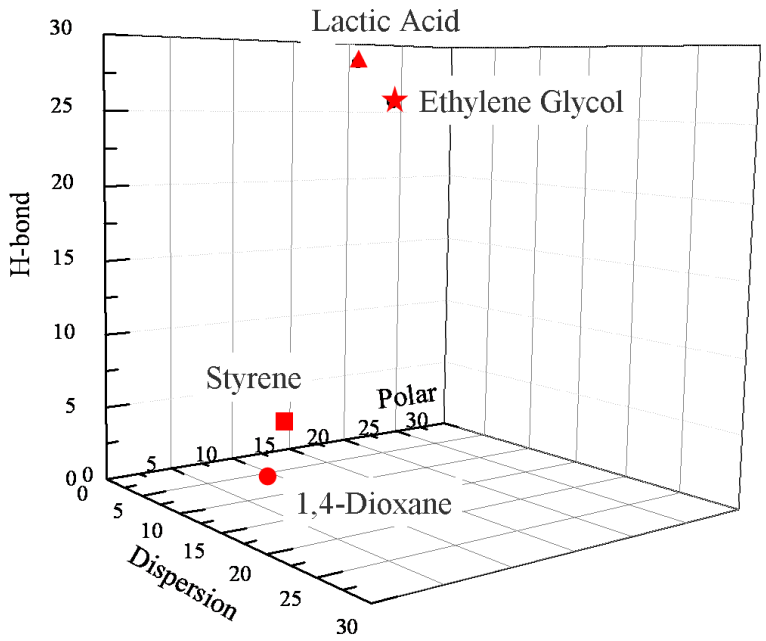

Figure 9 Hansen space: a 3-D coordinate system with the three axis corresponding to the dispersion parameter, dipole moment, and hydrogen bond.

References

1. Fukasawa, T.; Deng, Z. Y.; Ando, M.; Ohji, T.; Kanzaki, S., Synthesis of porous silicon nitride with unidirectionally aligned channels using freeze-drying process. *Journal of the American Ceramic Society* **2002,** 85, (9), 2151-2155.

2. Nishihara, H.; Mukai, S. R.; Yamashita, D.; Tamon, H., Ordered macroporous silica by ice templating. *Chemistry of Materials* **2005,** 17, (3), 683-689.

3. Zhang, H.; Cooper, A. I., Aligned porous structures by directional freezing. *Advanced Materials* **2007,** 19, (11), 1529-1533.

4. Kim, J. W.; Taki, K.; Nagamine, S.; Ohshima, M., Preparation of poly(L-lactic acid) honeycomb monolith structure by unidirectional freezing and freeze-drying. *Chemical Engineering Science* **2008,** 63, (15), 3858-3863.

5. Hua, F. J.; Park, T. G.; Lee, D. S., A facile preparation of highly interconnected macroporous poly(D,L-lactic acid-co-glycolic acid) (PLGA) scaffolds by liquid-liquid phase separation of a PLGA-dioxane-water ternary system. *Polymer* **2003,** 44, (6), 1911-1920.

6. Kim, J. W.; Taki, K.; Nagamine, S.; Ohshima, M., Preparation of Porous Poly(L-lactic acid) Honeycomb Monolith Structure by Phase Separation and Unidirectional Freezing. *Langmuir* **2009,** 25, (9), 5304-5312.

7. Ma, P. X.; Zhang, R. Y., Microtubular architecture of biodegradable polymer scaffolds. *Journal of Biomedical Materials Research* **2001,** 56, (4), 469-477.

8. Schoof, H.; Apel, J.; Heschel, I.; Rau, G., Control of pore structure and size in freeze-dried collagen sponges. *Journal of Biomedical Materials Research* **2001,** 58, (4), 352-357.

9. Ding, S. Q.; Zeng, Y. P.; Jiang, D. L., Fabrication of mullite ceramics with ultrahigh porosity by gel freeze-drying. *Journal of the American Ceramic Society* **2007,** 90, (7), 2276-2279.

10. Koch, D.; Andresen, L.; Schmedders, T.; Grathwohl, G., Evolution of porosity by freeze casting and sintering of sol-gel derived ceramics. *Journal of Sol-Gel Science and Technology* **2003,** 26, (1-3), 149-152.

11. Mukai, S. R.; Nishihara, H.; Shichi, S.; Tamon, H., Preparation of porous TiO2 cryogel fibers through unidirectional freezing of hydrogel followed by freeze-drying. *Chemistry of Materials* **2004,** 16, (24), 4987-4991.

12. Mukai, S. R.; Nishihara, H.; Tamon, H., Formation of monolithic silica gel microhoneycombs (SMHs) using pseudosteady state growth of microstructural ice crystals. *Chemical Communications* **2004**, (7), 874-875.

13. Nishihara, H.; Mukai, S. R.; Tamon, H., Preparation of resorcinol-formaldehyde carbon cryogel microhoneycombs. *Carbon* **2004,** 42, (4), 899-901.

14. Deville, S.; Saiz, E.; Nalla, R. K.; Tomsia, A. P., Freezing as a path to build complex composites. *Science* **2006,** 311, (5760), 515-518.

15. Deville, S.; Saiz, E.; Tomsia, A. P., Freeze casting of hydroxyapatite scaffolds for bone tissue engineering. *Biomaterials* **2006,** 27, (32), 5480-5489.

16. Araki, K.; Halloran, J. W., Room-temperature freeze casting for ceramics with nonaqueous sublimable vehicles in the naphthalene-camphor eutectic system. *Journal of the American Ceramic Society* **2004,** 87, (11), 2014-2019.

17. Fukasawa, T.; Ando, M.; Ohji, T.; Kanzaki, S., Synthesis of Porous Ceramics with Complex Pore Structure by Freeze-Dry Processing. *Journal of American Ceramic Society* **2001,** 84, (1), 230-232.

18. Fukasawa, T.; Deng, Z. Y.; Ando, M.; Ohji, T.; Goto, Y., Pore structure of porous ceramics synthesized from water-based slurry by freeze-dry process. *Journal of Materials Science* **2001,** 36, (10), 2523-2527.

19. Koh, Y. H.; Song, J. H.; Lee, E. J.; Kim, H. E., Freezing dilute ceramic/camphene slurry for ultra-high porosity ceramics with completely interconnected pore networks. *Journal of the American Ceramic Society* **2006,** 89, (10), 3089-3093.

20. Moon, J. W.; Hwang, H. J.; Awano, M.; Maeda, K.; Kanzaki, S., Preparation of dense thin-flm solid electrolyte on novel porous structure with parallel pore channel. *Journal of the Ceramic Society of Japan* **2002,** 110, (5), 479-484.

21. Mukai, S. R.; Nishihara, H.; Tamon, H., Morphology maps of ice-templated

silica gels derived from silica hydrogels and hydrosols. *Microporous and Mesoporous Materials* **2008,** 116, (1-3), 166-170.

22. Gutierrez, M. C.; Garcia-Carvajal, Z. Y.; Hortiguela, M. J.; Yuste, L.; Rojo, F.; Ferrer, M. L.; del Monte, F., Biocompatible MWCNT scaffolds for immobilization and proliferation of E. coli. *Journal of Materials Chemistry* **2007,** 17, (29), 2992-2995.

23. Chino, Y.; Dunand, D. C., Directionally freeze-cast titanium foam with aligned, elongated pores. *Acta Materialia* **2008,** 56, (1), 105-113.

24. Waschkies, T.; Oberacker, R.; Hoffmann, M. J., Control of Lamellae Spacing During Freeze Casting of Ceramics Using Double-Side Cooling as a Novel Processing Route. *Journal of the American Ceramic Society* **2009,** 92, (1), S79-S84.

25. Kim, J. W.; Tazumi, K.; Okaji, R.; Ohshima, M., Honeycomb Monolith-Structured Silica with Highly Ordered, Three-Dimensionally Interconnected Macroporous Walls. *Chemistry of Materials* **2009,** 21, (15), 3476-3478.

26. Kim, J. K.; Taki, K.; Ohshima, M., Preparation of a unique microporous structure via two step phase separation in the course of drying a ternary polymer solution. *Langmuir* **2007,** 23, 12397-12405.

27. Cui, L.; Han, Y., Honeycomb Pattern Formation via Polystyrene/Poly(2-vinylpyridine) Phase Separation. *Langmuir* **2005,** 21, (24), 11085-11091.

28. Hansen, C. M., ”Hansen Solubility Parameters: A User’s Handbook”, *CRC Press. Inc.*, **1999**